ELSEVIER

Contents lists available at ScienceDirect

Construction and Building Materials

journal homepage: www.elsevier.com/locate/conbuildmat





Feasibility of portable NIR spectrometer for quality assurance in glue-laminated timber production

Jakub Sandak ^{a,b,*}, Peter Niemz ^{c,d,e}, Andreas Hänsel ^f, Juana Mai ^{d,f}, Anna Sandak ^{b,g}

- ^a Andrej Marušič Institute, University of Primorska, Koper, Slovenia
- ^b InnoRenew CoE, Izola, Slovenia
- c ETH Zürich, Zürich, Switzerland
- ^d Bern University of Applied Sciences, Biel, Switzerland
- ^e Division of Wood Science and Engineering, Luleå University of Technology, Skelleteå, Sweden
- f Department of Wood and Wood-Based Materials, Saxon University of Cooperative Education, Dresden, Germany
- g Faculty of Mathematics, Natural Sciences and Information Technologies, University of Primorska, Koper, Slovenia

ARTICLE INFO

Keywords: Near infrared spectroscopy Glue-laminated timber Glulam Delamination Quality assurance

ABSTRACT

The feasibility of a portable NIR sensor for off-line determination of diverse wood quality aspects relevant in the production of glue-laminated timber was demonstrated. The best performance was noticed for assessing wood moisture content, with a lower capacity to estimate wood density and mechanical properties. NIR spectroscopy was modestly capable of predicting surface roughness. However, the traceability of the raw resources and the automatic classification of diverse wood defects were successfully demonstrated. The developed chemometric model could predict the total delamination and detailed delamination length. Finally, recommendations regarding further system development were provided with the aim of implementation and integration of the NIR measurement into glue-laminated timber production plants.

1. Introduction

Certified glulam is an accepted term for a composite with at least four timber lamellae glued together that were manufactured, controlled and marked according to certain rules. Glulam consists of individual layers of structural timber, providing a highly effective utilization of the raw material. Individual lamellae can be end-jointed by the process of fingerjointing to produce long lengths following the requirements of the relevant standard. One of the greatest advantages of glulam is that it can be manufactured in a wide variety of shapes, sizes and configurations to provide elements for wide-span but light construction [1]. The constitutive lamellae of the glulam are finger-jointed to create long components that are afterwards glued together to produce the desired size elements. Engineering of very large structural components (both thick and long) is possible considering the state-of-the-art production technologies, including computer-aided design of timber structures [2], innovative gluing solutions [3], integration of computer numerical control machines and robots [4], or use of modified timber [5] for glulam production. Glulam manufactured following the rules given in national or European codes is graded in pre-defined strength classes. The appropriate class is determined by the strength of the constitutive timber

used and its position within the cross-section. The resulting strength and stiffness values of various strength classes are then determined according to the code. The European standard EN 14080 [6] specifies the requirements for glue-laminated timber products used in load-bearing structures and deviations from target size corresponding to tolerance class requirements [7]. A critical glulam property directly affecting the service life expectation of timber structures is its vulnerability for cracking and delamination. Marra [8], Vanya [9], and Knorz [10] listed the following factors influencing the extent of cracking in glulam beams:

- environmental conditions, such as variation of the ambient air relative humidity or other cyclic changes of climatic conditions,
- material intrinsic properties, such as wood species, density, presence
 of extractives, grain or ring orientation, differences of the moisture
 content within/between lamellae, or different thicknesses of the
 lamellae causing inner stresses,
- adhesive properties, including resin quality, chemical composition, resistance at wet stage (e.g., during delamination test EN 391 [11] or A4 test according to EN 302-1 [12]),

^{*} Corresponding author at: InnoRenew CoE, Livade 6, 6310 Izola, Slovenia.

production parameters, for instance, pressure during curing, adhesive application method, pressing parameters, curing time, presence of primers or other additives.

An extensive review of diverse factors influencing the performance of the glue-laminated timber has been recently presented by Hänsel et al. [3]. Knorz [10] defined the delamination test as a rapid method to predict bond durability of laminated timber under exterior service. This testing approach was first developed by Truax and Selbo [13] who correlated the extent of delamination in the glue-laminated timber elements exposed to long-term (4 years) exterior weathering with delamination results of the laboratory tests. The matching samples of glued wood were treated there in a sequence of vacuum-pressure water impregnation and soaking-drying cycles. The general objective of such a test was to induce extreme stresses within the bond line that are equivalent to those occurring in the real elements during the service life of a timber structure. The experimental protocol was further elaborated to limit the test duration to three days only [14]. Such testing procedure was a basis to define a standardized evaluation process used routinely for the assessment of adhesives intended for gluing laminated timber for exterior exposure applications. The latest versions of standards allow both evaluation of the suitability of adhesives for structurally laminated wood [15,16] as well as quality control of the glulam production directly in the factory [6].

An appropriate delamination testing procedure should be applied depending on the service class foreseen for the end-product [17,18]. It should also include an analysis of the risk levels associated with the use of the given structural component. The objective of the delamination test is to create stresses in the bond line by saturation of the sample in water beyond the fibre saturation point followed by a quick drying. The failure observed, usually as a glue bond delamination, occurs when the bond quality is insufficient. The length of the opening in relation to the nominal length of the bond line is called the delamination ratio and is used to express the bond quality. The European standard EN 302-2 comprises the testing methods suitable for the assessment of glued members used in interior and/or exterior [16]. Test protocols vary concerning the growth tree ring alignment, glued lamella thickness, and drying conditions (temperature and humidity). The selection of the specific settings depends on the assessed adhesive type. The soaking of wood in water is performed at temperatures of 20 to 25 °C under cycles of vacuum (25 \pm 5 kPa) followed by high-pressure water impregnation (600 \pm 25 kPa). The drying stage can be performed either at 65.0 \pm 3.0 °C or at 27.7 \pm 2.5 °C. Three soaking / high-temperature drying cycles are applied for adhesive type I to be used in service classes 1, 2 and 3 [19]. Only two cycles at low drying temperature are used for other glues. The mild testing protocol can be useful to test glued wood members exposed to indoor conditions. It was reported that wood delamination is often noticed within very dry climates, typical for heated rooms, where relative humidity can reach values below 20% during the winter season [20]. The delamination D is calculated according to equation (1):

$$D = \frac{L_1}{L_2} \cdot 100\% \tag{1}$$

where L_1 – total delamination length, L_2 – total length of the bond lines. Both properties are measured at the end grain surfaces and expressed in mm.

The standard EN 1995-1-1:2004 [19] requires that timber used to manufacture glulam is strength graded either visually or mechanically. However, the strength class to which a glulam member is assigned depends not only on the grade of the constitutive timber lamellae but also on the build-up of the glulam section. The standard EN 1194:1999 [21] defines the set of characteristic glulam properties required for designing timber structures according to Eurocode 5. The glulam can be "homogenous" or "combined". In the first case, all of the constitutive

lamellae are graded as the same strength class. Conversely, the outer lamellae are of higher strength than the inner in the case of combined glulam components [1]. Manufacturing of glue-laminated timber and minimum production requirements are defined in EN 385 [22]. The difference in moisture content between individual laminates within a single glulam element should not exceed 4 % (EN 386) [23]. The specific requirements for structural adhesives are listed in EN 301 [24]. Mechanical properties of glue-laminated timber components should be assured by experimental procedures prescribed in EN 408 [25]. The strength-class grading can be based on experimental testing results following EN 408. Alternatively, the strength-class can be assigned by implementing the specific calculation procedure and considering the mechanical properties of the laminated timber lamellae used in production. Even if precisely defined in the standard, the practical implementation of quality assurance at the factory floor is far more complicated.

Several technologies have recently been introduced by the wood industry to assure product quality control. The optimal use of the material and the quality inspection of final products have a significant impact on the production economy, sustainable use of the raw resources, and the overall satisfaction of the final customers. Quality assurance is often considered as an additional cost to production, requiring additional resources and time for proper implementation. Initially, these inspections were carried out by trained operators based on visual assessment. Such a solution is highly problematic due to its subjective nature and several limitations associated with the training level, concentration ability of inspectors, among others. Nowadays, developments in the field of optics and electronics allow the replacement of human inspection by technologies with a high degree of performance [26]. Diverse industrial scanners become an integral part of advanced manufacturing solutions in the wood industry, allowing material sorting, grading or process optimization [27,28]. Techniques adopted for scanners include diverse techniques measuring the interaction of the electromagnetic waves (x-ray, ultraviolet, visible light, infrared, or microwaves) as well as acoustic waves, such as sound or ultrasound. Among those, near infrared spectroscopy (NIR) is a particularly promising technology for industrial use due to its non-destructive character and fast measurement principle [29].

Several successful implementations of Fourier-transform near infrared (FT-NIR) spectroscopy for the determination of diverse wood properties were reported by numerous authors [30–34]. Campos et al. [35] used FT-NIR to evaluate the composition of agro-based particleboards. Sandak et al. [36] reported the application of FT-NIR spectroscopy for the development of an expert system capable of particleboard classification. Portable low-cost spectrometers were successfully utilized for the detection of wood defects [37]. The quality control of adhesives used for the production of wood-based composites was tested from the NIR spectroscopy perspective. Meder et al. [38] presented an at-line measurement system for the quality control of melamine-urea-formaldehyde resin in the production of composite wood panels. Taylor and Via [39] used VIS-NIR spectroscopy to quantify phenol-formaldehyde resin content in oriented strandboards. The solid content of amino resins was determined with NIR spectroscopy by Gonçalves et al. [40]. An attempt for identification of spectral changes of the adhesive related to ageing, curing temperature, or preservative treatment of the glued wood was reported by Gaspar et al [41]. Pemberger et al. [42] used NIR to monitor the curing process of silicone adhesives. Tomlinson et al. [43] demonstrated the feasibility of spectroscopy in mid-infrared (IR) and NIR ranges for monitoring the curing process of cyanoacrylates. Even if several examples of successful NIR implementation for product and process quality monitoring have been reported, most of them rely on Fourier transform near infrared spectroscopy (FT-NIR) instruments possessing the highest spectral resolution and providing spectra covering a broad wavelength range. The FT-NIR technique is relatively costly (both time and investment-wise) and with limited applicability for in-factory or at-line measurements. It is

related to the fragile nature of interferometers used for modulating infrared light. For that reason, an alternative to FT-NIR spectroscopy is of great interest for wood-working industries. There are several technical solutions potentially applicable, including; diffraction-based spectrometers, micro-electro-mechanical systems (MEMS), linear variable filters (LVF), acousto optic tunable filters (AOTF), dispersive monochromators (DM), dispersive fixed grating diode arrays (DA), among others [36].

Portable spectroscopic equipment operating in the NIR range of electromagnetic radiation seems to be an especially interesting technology for the wood-based sector [34]. Such instrumentation could assist the rapid assessment of critical material properties in a non-destructive, accurate and rapid manner. MicroNIR spectrometer produced by VIAVI demonstrated superior performance in the assessment of biological materials in the field of agriculture [44,45], food production [46–48], rapid plastic waste sorting [49], and recycling of polymer commodities [50]. For that reason, it was identified as a sensor solution potentially applicable for the assessment of engineered wood products, such as glulam.

Besides the hardware used for the acquisition of the representative spectra, the spectra processing algorithms, as well as chemometric models used for qualification and/or quantification, are equally important [34]. It is particularly challenging in the case of biological materials such as wood, where its native heterogeneity, anisotropy and hygroscopic properties require sophisticated data processing solutions and a high number of replicates to assure reliable predictions. The most common implementation of chemometric models relies on the partial least squares (PLS) method where reference values of the predicted property are regressed against latent variables derived from the NIR spectra. This method usually provides optimal prediction performance and allows interpretation of the variables' contribution to the model. As an alternative, machine learning algorithms are becoming popular nowadays increasing, even more, the prediction capability of NIR systems implemented in diverse applications. A limitation of such solutions is its "black box" nature, limiting interpretability of the neuron weights meaning, as well as a very high number of training data indispensable to generate a reliable model [51].

The goal of this research was to investigate the feasibility of a portable NIR sensor (MicroNIR) for the off-line determination of diverse wood quality aspects that are relevant in the production of glue-laminated timber. A special focus was on the preparation of chemometric models linking acquired spectra with data collected by means of reference methodologies. Such a measurement approach can be highly useful in the quality sorting of timber, where several critical (for appropriate glue bond resistance) wood properties are assessed at once with a single measurement. The early knowledge of wood suitability can substantially contribute to improve the quality assurance of the engineered wood used in timber construction and, consequently, increase user confidence in such sustainable technologies.

2. Materials and method

2.1. Investigated wood

Materials used for characterization included beech (*Fagus silvatica*) wooden boards provided by the Swiss company neue Holzbau AG (Lungern, Switzerland). The declared origin of wood was Switzerland. The moisture history included conventional kiln drying followed by airdry storage in the factory conditioning room. The wood was warehoused for at least six months to assure relaxation of internal stresses and moisture content equilibration. All the raw boards used in the experiment were preselected to include a broad assortment of wood quality aspects and to cover a wide range of wood densities. Experimental samples were selected and prepared to represent six alternative experimental scenarios:

- I. standard quality wood, rotary planed with sharp knives
- II. poor quality wood (containing defects), rotary planed with sharp knives
- III. standard quality wood, rotary planed with a dull knives
- IV. standard quality wood, sanded with P100 sanding paper
- V. wooden lamellae at varying moisture contents
- VI. standard quality wood, rotary planed with sharp knives and coated with a primer before gluing

The protocol for the experiment implementation is shown in Fig. 1, including the list of variables collected along the process. A set of 29 raw boards was first selected with the support of the industrial partners to identify beach boards representing various quality materials, which are used in the daily production of glue-laminated timber products. Each board was ID marked and quality graded following visual assessment and stress grading through Mechanical Timber Grader MTG (Brookhuis Micro-Electronics, Enschede, the Netherlands). In addition, external dimensions were measured, and the presence of wood defects was detected on each board. Experimental samples (n = 114) were cut out from raw boards with a cross-cutting circular saw to extract elements of 650 mm length. The information regarding the raw board ID was preserved by marking each sample with a proper code. A whole lot of experimental samples was transported to Bern University of Applied Science (Biel, Switzerland) for final conditioning and sizing. The dimensions of experimental samples after sizing were 150 \times 28 \times 500 mm^3 (width \times thickness \times length, respectively). The majority of samples (n = 98) were stored in an air-conditioned storage room at a temperature of 20 °C and 46% air relative humidity (RH). A set of beech samples (n =20) containing diverse wood defects (knots, bark pockets, discolorations or fibre deviations) was selected from the whole sample collection. In addition, one subset (n = 8) of samples was conditioned at 50 °C, 40% RH, while a second subset (n=8) at 20 °C and 65% RH. The resulting moisture content (MC) after conditioning was measured with a pin moisture meter (PCE Inst., Durham, United Kingdom) in at least five boards from each lot. Measured MC corresponded to 4%, 7% and 15% for dry (40% RH), normal (46% RH) and wet (65%) storage conditions, respectively. The wood density was determined for each conditioned experimental sample by measuring its dimensions and weight at the equilibrium moisture content state.

2.2. Preparation of glued wood surfaces

The final surface preparation of the samples' glued areas was performed on standard woodworking machines following pre-defined experimental scenarios. A new set of cutting knives was installed on the thickness planer D632 (Hofmann, Bad Windsheim, Germany) to generate a set of samples with a smooth, planed surface (n = 74), including wood samples with defects and foreseen for primer application (scenario I, II, V, VI). In the next step, an old set of cutting knives was installed on the same planing machine and additionally wearied by rough planing of particle boards. Such prepared tools were utilized for the generation of "dull-tool surfaces" on n = 20 beech wood samples (scenario III). Finally, a subset of n = 20 experimental samples was sanded on the wide belt sanding machine Sandeq W-200 (Homag, Schopfloch, Germany) with P100 abrasive paper to generate samples for the "sanded surface" scenario IV. The final thickness of wood after machining of both sides was 25 mm. The resulting surface roughness was measured at that stage utilizing stylus profilometer Surftest SJ-210 (Mitutoyo, Kawasaki, Japan) with a tip radius of 5 µm and tip angle of 90°. The cut-off wavelength was $\lambda=2.5$ mm and scanning length 12.5 mm. At least three measurements were performed on each surface along and across fibre directions with a scanning speed of $0.5~\mathrm{mm\cdot s}^{-1}$. A whole portfolio of surface roughness parameters was recorded, but only average roughness Ra computed as an average of measurements across fibres was used for analysis. NIR spectra were acquired in parallel to the surface roughness measurement according to the procedure described in

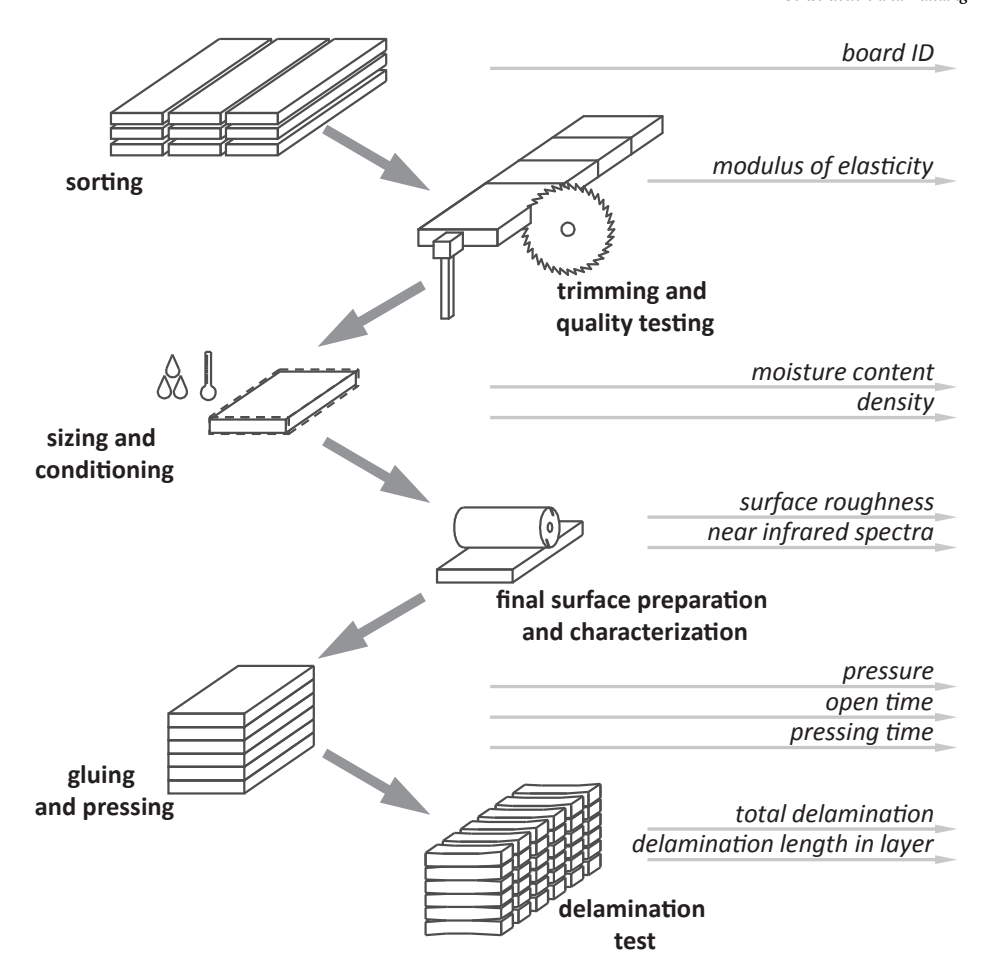


Fig. 1. Steps for preparation of experimental samples for delamination tests and collection of wood/gluing process properties.

the section 2.5.

2.3. Gluing of wood samples

Experimental samples were used for the preparation of the gluelaminated timber blocks used for the determination of the glue bonds resistance for delamination. Special care was directed to minimize the time after surface preparation and glue application. Therefore, the time between wood surface machining and pressing operation was less than 3 h. A protocol described in EN 302–2:2017 [16] was implemented here. The set of 6 wooden boards replicated three times was used for each experimental scenario. In total, 18 (6 scenarios × 3 replicas) blocks were obtained after gluing wood with one-component polyurethane adhesive 1C PUR. The glue was applied on the pre-defined sides of five boards. The last (sixth board) was not covered by glue layer but added to the set before installation in the press. The open time of this adhesive defined by the producer is 30 min, while the pressing time is 75 min. The application rate of the glue was 0.18 kg/m² and followed the producer's recommendations. All glued surfaces of one set of wooden boards (scenario VI) were coated with a primer provided by the adhesive producer (the chemical solution was not revealed). The primer application was manual using the spray with a rate of 0.02 kg·m⁻². The primer was applied on all surfaces involved in the bonding, including external lamellae on one side and internal lamellae on both sides. The specific pressure of the press was set at 1.0 MPa and the pressing time was extended to 600 min to assure optimal curing conditions. The temperature of the press was not controlled, and the process of glue hardening was in room conditions (24 $^{\circ}$ C, 55% RH). Glued blocks were extracted from the press and left for one week to release stresses.

It should be mentioned that n = 108 wooden pieces were used for

gluing experimental blocks, compared to n=114 selected from the source boards. The remaining pieces were used for additional experiments such as calibration of models predicting wood moisture content.

2.4. Delamination test

Glued blocks of experimental wood samples were processed after conditioning to select six pieces of standardized samples used for the delamination test. The final size of each sample after processing was 145 \times 150 \times 75 mm 3 (width \times height \times length, respectively). No sign of delamination was observed after such manufacturing of samples. The delamination test followed EN 302–2:2017 [16] and consisted of the following stages:

- Installation of experimental samples in the autoclave
- • Impregnation of the samples by water under vacuum (25 \pm 5 kPa, 20 \pm 5 °C) for 15 min
- \bullet Further impregnation with water in elevated pressure conditions (600 \pm 55 kPa, 20 \pm 5 °C) for 60 min
- An additional cycle of the 15 min vacuum and 60 min high-pressure impregnation
- Installation of impregnated samples in the climatic chamber
- \bullet Drying of wood for 20 \pm 2 h at 65 \pm 3 °C and 12% $\pm 3\%$ RH at the atmospheric pressure

The glue bond delamination was assessed visually and measured with a millimetre scale, separately for each glue line layer on both cross sections of every sample. In addition, a total delamination index was computed for each sample replica as an average ratio of the delamination length to the total glue line length.

2.5. NIR spectra measurement

The sensor selected for NIR spectra acquisition was the MicroNIR OnSite-W spectrometer (VIAVI Solutions Inc. (Milpitas, CA, USA)) [52]. It is a portable spectrometer that has integrated all optical components necessary for NIR spectra acquisition. The MicroNIR uses a linear variable filter for wavelength segregation and a 128-element InGaAs array as the photodetector. The spectral information is represented as 128 values measured in the range from 1000 to 1700 nm. Two vacuum halogen micro lamps are implemented as the source of infrared light. An advantage is that no extra time is necessary for warming up the lamp to stabilize the reading of the instrument as this solution allows immediate emission of the full light power after switching on. The instrument was manually operated with software MicroNIR $^{\mbox{\tiny TM}}$ Pro v3.0 provided by the sensor producer. The software was installed on a portable computer where all acquired spectra were stored. The communication between sensor and PC was with Bluetooth interface and allowed wireless operation. The battery installed in the sensor allowed continuous operation

The procedure for NIR spectrum acquisition included white (100% reflectance) and black (0% reflectance) reference measurements performed with a dedicated accessory (Spectralon resin). The reference scanning was repeated every 10 min of operation. A frequent white and black reference acquisition was performed to minimize the drift of spectra due to temperature changes of the semiconductor InGaAs detector. Spectra were collected from the wood surface by placing the sensor on the measured spot and triggering the acquisition by pressing the button on the MicroNIR spectrometer (Fig. 2). Each studied board was assessed on both length sides, assuring measurement of at least 5 points located randomly on each board side.

2.6. Data evaluation

Custom software was developed in LabView 2019 (National Instruments, Austin, TX, USA) for post-processing of NIR spectra. Normalization of the spectra collected from each side of the scanned board (5 measurements) were routinely implemented utilizing Extended Multiplicative Scatter Correction (EMSC) [53]. It allowed the removal of the non-uniform scatter effect due to wood heterogeneity and variation of the surface roughness. In the next step, all EMSC normalized spectra from each side of the experimental board were averaged. As a result, a total of 216 spectra were available for analysis, considering 6 scenarios \times 3 replica/scenario \times 6 bonded lamellae/replica \times 2 sides/bonded lamella \times 1 (of 5 averaged) spectrum/side. The calibration set was formed by adopting all measurements for replica #1 and #2, while the validation spectra set included data from the remaining replica #3. It



 $\begin{tabular}{ll} Fig. \ 2. \ MicroNIR \ OnSite-W \ sensor \ used \ for \ off-line \ manual \ acquisition \ of \ NIR \ spectra. \end{tabular}$

resulted in 67% of samples used for calibration and 33% for independent validation.

The PLS_Toolbox (Eigenvector Research Inc., Manson, WA, USA) and Matlab R2020 (MathWorks, Inc., Natick, MA, USA) were used for chemometric models development. EMSC, Standard Normal Variate (SNV), Orthogonal Signal Correction (OSC) [54], Savitzky-Golay 1st and 2nd derivatives [55] (window size 11), and vector normalization were used as alternative spectra pre-processing routines for data preparation before modelling. Principal Component Analysis (PCA) was applied for explorative analysis of raw spectra and identification of all outliers or wrongly measured spectra. Partial Least Squares regression was implemented for quantitative analysis. NIR spectra were used for the determination of the material properties represented as a reference data set measured through dedicated protocols in parallel to spectroscopic assessment. Furthermore, it was possible to link each NIR spectrum with the original longboard (before cut-to-length operation) and its quality class assigned by the industrial experts. In that case, Partial Least Squares - Discriminant Analysis (PLS-DA) were performed for the determination of the original board number. A similar approach was also used for the identification of diverse wood defects studied in one experimental scenario. For that reason, special care was directed toward the assessment of abnormal wood, where a supplementary database of NIR spectra was collected for further PLS-DA discriminant analysis.

The model development included cross-validation with venetian blinds and 10 data splits. The number of latent variables (LV) tested during calibration varied from 2 to 10. The best configuration was determined by analysis of the cross-validation results represented as the value of root mean square error of cross-validation (RMSECV) combined with the explained variance analysis. Therefore, the number of LV was decided as a compromise between the smallest RMSECV and relevant variance explained (>1%). Each chemometric model presented below is a result of an optimization procedure implemented with a dedicated software tool (model optimizer), being part of the PLS_Toolbox. The optimization included confrontation of diverse PLS model configurations, number of LV, pre-processing algorithms and spectral bands used. The model with the smallest root mean squares error of prediction (RMSEP) and simultaneously with a low number of LV was considered optimal. In addition, the determination coefficient for calibration and validation ($R^2(cal)$ and $R^2(val)$) and the related ratio of performance to deviation (RPD) were considered important quantifiers of the chemometric models' quality.

3. Results and discussion

The portable NIR spectroscopy was tested in this research toward understanding its feasibility in diverse tasks relevant when producing glue-laminated timber beams. A key question was if a single measurement of NIR spectrum can be sufficient for tracking the raw resources, prediction of relevant mechanical or physical properties, identification of surface characteristics, as well as the projection of the glue bond resistance. The following chapters will provide results from a series of separate experiments focused on testing the above-mentioned functionalities.

3.1. Source board identification

All experimental beech wood samples used for gluing tests (n=108) were originated from 37 different source boards. It was stated by the production engineers at neue Holzbau AG that tracing boards along the production process would be an interesting functionality of NIR spectroscopy. The specific set of chemical/physical properties unique for each living tree, defined as a "fingerprint", is preserved in all boards extracted from that tree. Every wooden board can, therefore, be traced along the supply chain if it properly recognizes its individual "fingerprint". A dedicated PLS-DA model was built to investigate the feasibility of this approach. Only samples used in scenarios I, III, IV and VI were

applied for source board tracking to minimize variance related to the abnormal wood presence (II) and/or differences in wood moisture content (V). Finally, a set of 144 spectra corresponding to 29 source boards was extracted from the data set with each board represented by two spectra corresponding to two longitudinal sides of each board as measured with the NIR spectrometer. The PLS-DA model was created assuming EMSC and mean centre as pre-processing. It was sufficient to use only 4 LV and spectral bands covering the whole range of MicroNIR sensors to reach a satisfactory result for this task. A resulting confusion matrix visualizing the performance of the algorithm in classification is presented in Fig. 3. It is evident that the NIR spectra properly recorded "fingerprint" for a great majority of tested source boards. Only a few false-negative and false-positive spectra were misclassified, providing overall success of classification for 128 among 144 spectra (success rate = 89%). It should be mentioned, however, that the "most probable" rule for the PLS-DA classification was implemented here. The classification success was lower when the "prediction strict" rule was applied, resulting in the majority of spectra being unassigned to any source board class. It is fully justified as the variance between different source boards is relatively small. Moreover, considering the fact that the detailed provenance for each tested board at the log level was not known, it was impossible to modify the definition of classes that may result in some reasonable misclassifications.

3.2. Classification of wood defects

Wood is a natural material derived from trees. Consequently, it includes all features that the living plant formed in addition to the regular wood during growth. It includes branches, abnormal wood tissues, or fungi-degraded wood, among many others. Although branches are vital for the growth of the tree, their remains in timber (knots) are considered a serious defect. Similarly, bark, pith, spiral grain, reaction wood or cracks are wood features negatively influencing the performance of glue-laminated components during production and service life [56]. It is important, therefore, to assure that the timber used for gluing is defectfree or within the allowed range of wood imperfections. A usual solution is to cut out zones containing defects detected by the specialized scanner and to reassemble the board by finger-joining [57]. Even if several commercial industrial scanner solutions are available for implementation in glue laminating production lines, the automatic detection and classification of wood defects is still a challenge. The majority of these scanners rely on vision, tracheid effect, laser triangulation, x-ray, microwave, or stress wave analysis [28]. NIR spectroscopy provides an

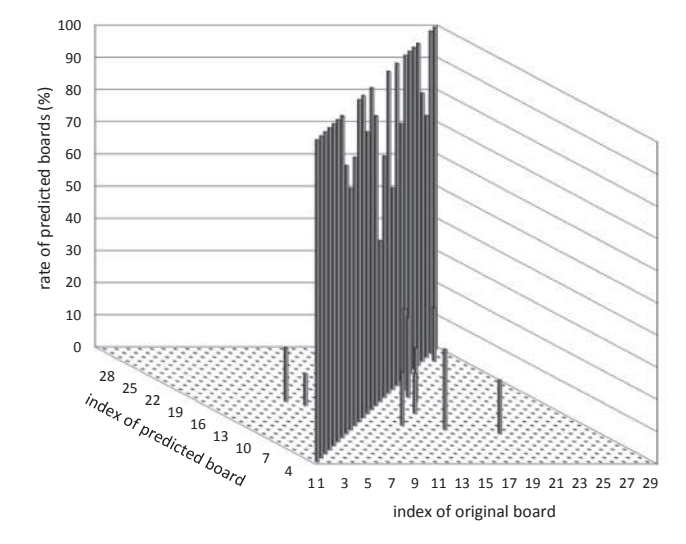


Fig. 3. PLS-DA discrimination beech wood boards used for tracing material along the glue-laminated timber production process.

alternative set of information that may complement state-of-the-art solutions, increasing the overall system performance [33].

A dedicated experiment scenario (IV) was designed to assess MicroNIR sensor capability to differentiate between normal and defected wood. An example of diverse wood defects present in studied wood samples is shown in Fig. 4. The list of assessed defects included: knots, pith, cracks, bark, and wet surface artificially moistened to simulate uneven wood moisture content. Each of those was measured by the spectrometer and the resulting spectra were analysed with a PLS-DA discrimination algorithm. The model performance is illustrated as a confusion matrix, where histograms of the properly and falsely classified spectra are plotted in Fig. 5.

In analogy to the board identification, perfect discrimination by the PLS-DA model appears as the diagonal of 100% accuracy indicating all samples properly discriminated. The model developed was capable to properly classify all kinds of defects, which was confirmed by the analysis of independent validation set results. The misclassification was noticed only in a few cases corresponding to the problematic measurement circumstances, such as a relatively small area of the defect that was smaller than the effective measurement area of the sensor. It was especially noticeable in the case of a pith that was confused with a knot and/or bark.

3.3. Prediction of wood density

Wood density is a key physical material property determining its technical suitability as a construction material, particularly gluelaminated timber [56]. Unfortunately, density cannot be measured directly from the NIR spectrum by linking to specific absorbance peaks or other spectral features [30,34]. It can be determined, therefore, only indirectly by interpreting the light scatter variations and/or linking to the general infrared light absorbance pattern of the main chemical components present in the woody polymer matrix. The reference density data corresponding to samples tested in this experiment covered a relatively wide range from 550 to 850 kg·m⁻³. The PLS model developed for the prediction of the wood density by analysing its spectra is presented in Fig. 6. The RMSEP = $33.4 \text{ kg} \cdot \text{m}^{-3}$ with determination coefficient $R^2 = 0.46$ indicate moderate model's performance [30]. Similar or even higher values of RMSEP were reported previously [58–61]. As in the case of all models reported here, the validation samples (highlighted in Fig. 6 as diamonds) were not included in the training data set (presented as black dots). It should be mentioned that surface characteristics of samples assessed varied as these were prepared according to scenarios I, III, IV and VI, corresponding to surfaces sanded and planed with sharp and dull knives. It introduces an additional source of variance and, consequently, alters the PLS model prediction capacity. Even with that, the optimal number of latent variables was small (LV = 4). Some related reports from other researchers demonstrate relatively better model performance than reported here [62,63]. However, most of this research was performed in the laboratory environment as well as assuring much



Fig. 4. Examples of beech wood boards containing wood defects detected with NIR spectroscopy.

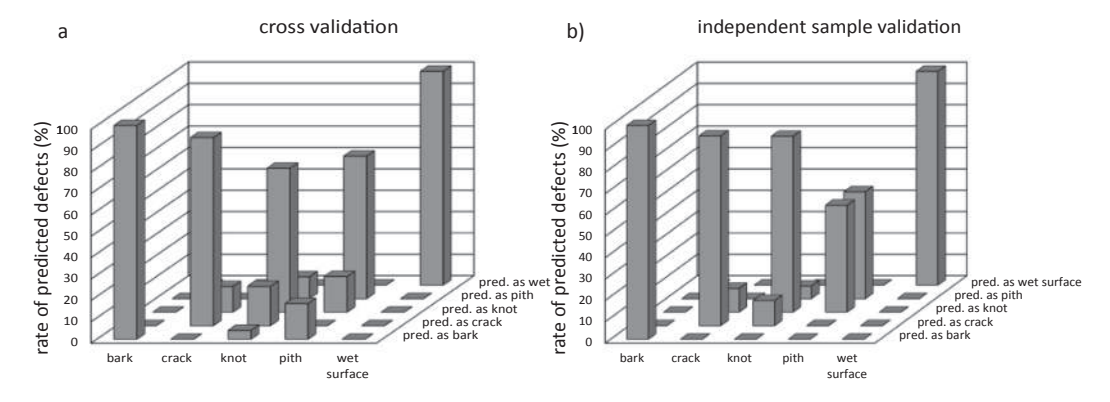


Fig. 5. Confusion matrixes for cross-validation (a) and independent sample validation (b) of the PLS-DA model used for identification of deficiencies in BEECH wood.

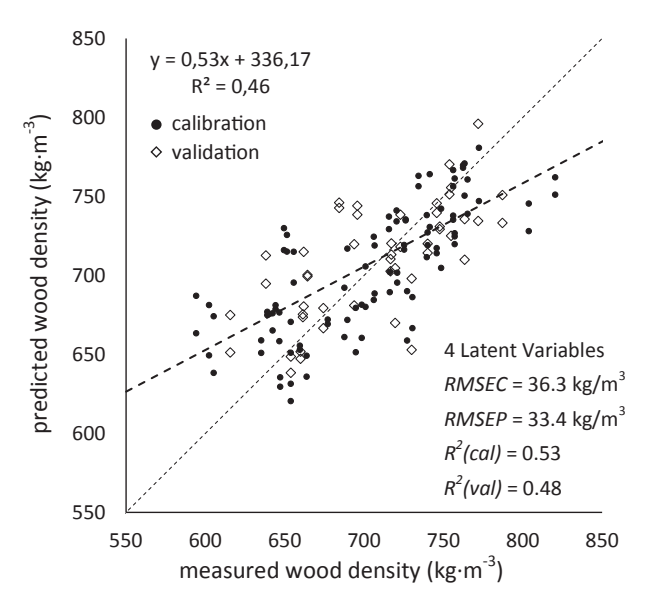


Fig. 6. Partial Least Square (PLS) chemometric model predicting the density of beech wood used for glue-laminated timber production. Note: The regression dashed line corresponds to the validation data set (open diamonds) and the diagonal point line indicates the perfect correlation trend.

more homogeneous surface topography than in the case of this experiment.

The regression of the validation points in the chart presented in Fig. 6 highlights a general problem of the PLS model related to the response flattening combined with a relatively high bias. An alternative to PLS regression algorithms was tested to search for a more reliable representation of the experimental data. A prediction capacity of the neural network model is presented in Fig. 7 as an example of such an alternative. Both the slope and intercept of the regression function are improved. However, even if *RMSECV* was noticeably reduced, the *RMSEP* was higher than in the case of PLS. It leads to the conclusion that the suitability of the neural network for practical applications was reduced. Also, it has to be mentioned that the number of training spectra available in this test was limited. The future calibrations with an extended dataset may result in dramatic improvement of the neural network model's performance [64].

3.4. Prediction of the wood mechanical properties

In analogy to density, NIR spectroscopy is not capable to assess the mechanical properties of materials through the direct spectra interpretation. Nevertheless, it was previously reported that chemometric models were successfully implemented for the determination of the

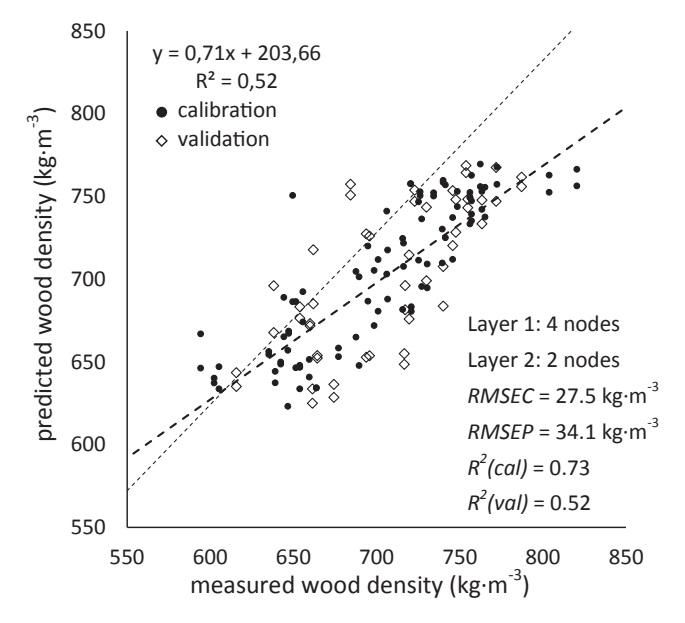


Fig. 7. Neural network (NN) model predicting the density of beech wood used for glue-laminated timber production. Note: The regression dashed line corresponds to the validation data set (open diamonds) and the diagonal point line indicates the perfect correlation trend.

Young modulus (MoE) among the other physical properties of wood [65]. A similar trial for linking NIR spectra with the dynamic MoE assessed on wooden board source was performed in this research. It should be mentioned that these tested boards had different dimensions and included embedded wood defects that were cut out when preparing samples used for gluing tests. It is an important limitation as global (whole board) mechanical properties were used as the reference values for calibration of the chemometric model with spectra set collected on smaller samples extracted from such boards. However, it was considered as the most practical solution reflecting real circumstances for the implementation of NIR spectroscopy toward industrial testing. The resulting PLS model is shown in Fig. 8, assuming the whole spectral range of the MicroNIR instrument used for model calibration. Orthogonal Scatter Correction (OSC) was applied as a pre-processing with the number of LV = 8 resulting from the model optimization procedure. The error of prediction was RMSEP = 947 MPa, which corresponds to less than $\pm 7\%$ of misrepresentation. Such a result is encouraging as the prediction capability may be further improved in the follow-up research when including a higher number of data points used for a model generation as well as more accurate linkage of the mechanical properties reference values with specific NIR spectra.

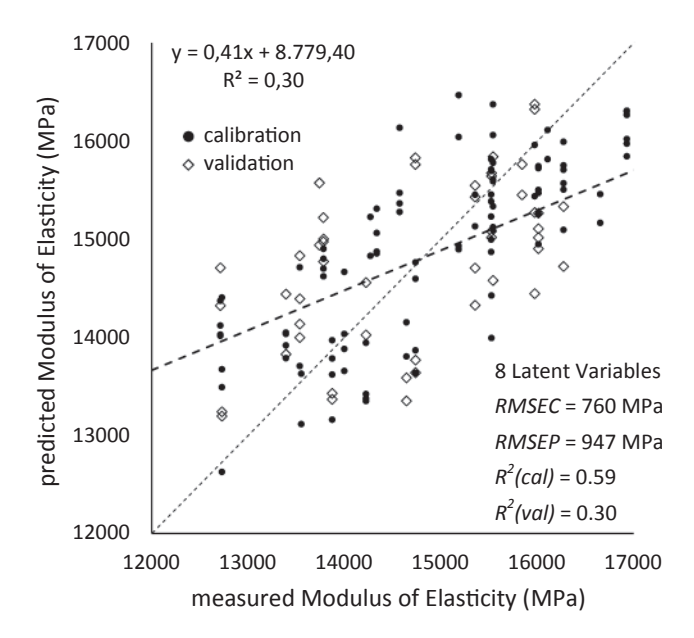


Fig. 8. PLS model for prediction of the mechanical properties of beech wood using NIR spectroscopy. Note: The regression dashed line corresponds to the validation data set (open diamonds) and the diagonal point line indicates the perfect correlation trend.

3.5. Prediction of wood surface roughness

The wood surface roughness is a material property recognized as highly influencing the glue bond strength [66,67] and, therefore, was assessed for the needs of this research. The roughness measurement methodology was implemented based on the surface profile acquisition through a stylus probe. It is commonly accepted as a standard solution, even if it possesses important limitations [68–70]. The contact nature of this system excludes its application toward in-line process control. Moreover, the measurement is relatively slow, which limits the number of characterized spots making the assessed value valid only for a specific location over the sample area. The possibility for a rapid assessment of the surface topography and, consequently, assurance of the superior glue bond quality is highly interesting for glue-laminated timber producers [71-73]. A chemometric model linking the average surface roughness (Ra) with the NIR spectra was created to identify the prediction feasibility. A resulting regression of measured values versus predicted by the PLS model is presented in Fig. 9. Samples from experimental scenarios I, III and IV (sharp and dull tool as well as sanding, respectively) were used for the model development. Extended multiplicative scatter correction was used as a spectrum pre-processing routine. Even if the calibration data points were regressed relatively accurately, the validation data were not distributed as expected along the diagonal of the chart. It is evidenced by the low value of the regression line slope = 0.36. A slight model tendency to overfit the data was recognized when combining a small slope with LV = 7 components found as an optimal configuration. The surface roughness prediction capacity of the MicroNIR sensor remains questionable, especially when considering the lack of a solid physical basis for interpreting links between infrared spectra absorbance and the surface topography expressed as roughness parameters.

3.6. Prediction of wood moisture content

Water is a polar molecule possessing a strong dipole momentum that is heavily absorbing infrared radiation, converting it into molecular vibrations. It is revealed in the NIR spectrum as pronounced absorbance peaks with height correlated to the quantity of water (or other hydroxyl functional groups) present in the subsurface of the measured material.

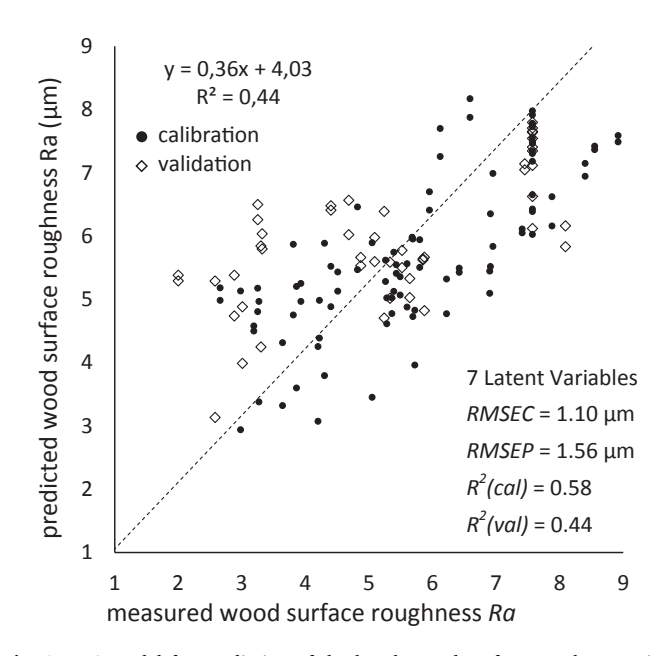


Fig. 9. PLS model for prediction of the beech wood surface roughness using NIR spectroscopy. Note: The regression dashed line corresponds to the validation data set (open diamonds) and the diagonal point line indicates the perfect correlation trend.

Near infrared spectroscopy was successfully implemented for the determination of the moisture content of diverse organic materials [74] including wood [30,61,75]. A dedicated chemometric model was developed for the needs of this research by measuring samples from scenario V. Following the experimentation protocol, a total of 18 wooden boards conditioned in three diverse climatic conditions were used for model preparation. Spectra collected on six of these boards were used for model validation. The average moisture content for each climate was used as a reference value for prediction. It resulted in the representation of the moisture content distribution creating three clusters shown in Fig. 10a. Even if both, small RMSEP and high R^2 , indicates relatively good performance, the resulting model was considered as rather weak, especially when referencing it to available literature references [30]. The recognized reasons are related to the error in reference values of moisture content. These were measured with a relatively inaccurate electrical resistance method and averaged to approximate the moisture content range. Moreover, a limited number of samples available, combined with the time passing between the collection of samples from the storage and NIR measurement resulted in an additional weakening of the reference values consistency. It triggered an additional experiment dedicated to the improvement of the chemometric model. In that case, the high number of samples (n = 250 pieces) obtained from the extra wooden boards not used for the gluing tests were conditioned in diverse climate conditions. It covered the equilibrium moisture content varying from 0 % to fibre saturation point (30 %). The small size of samples ($25 \times 25 \times 5 \text{ mm}^3$) assured uniform moisture distribution and fast response to the relative humidity changes. Finally, the moisture content was very precisely assessed using the standard gravimetric method linking the mass of embedded water related to the mass of dry wood. A high number of accurately assessed samples resulted in a superior moisture content prediction model as presented in Fig. 10b. The obtained error was RMSEP = 0.76% with the determination coefficient $R^2(val) = 0.99$. The number of latent variables LV = 5 indicates a low tendency of the model for data overfitting and indicates its high potential for practical applications.

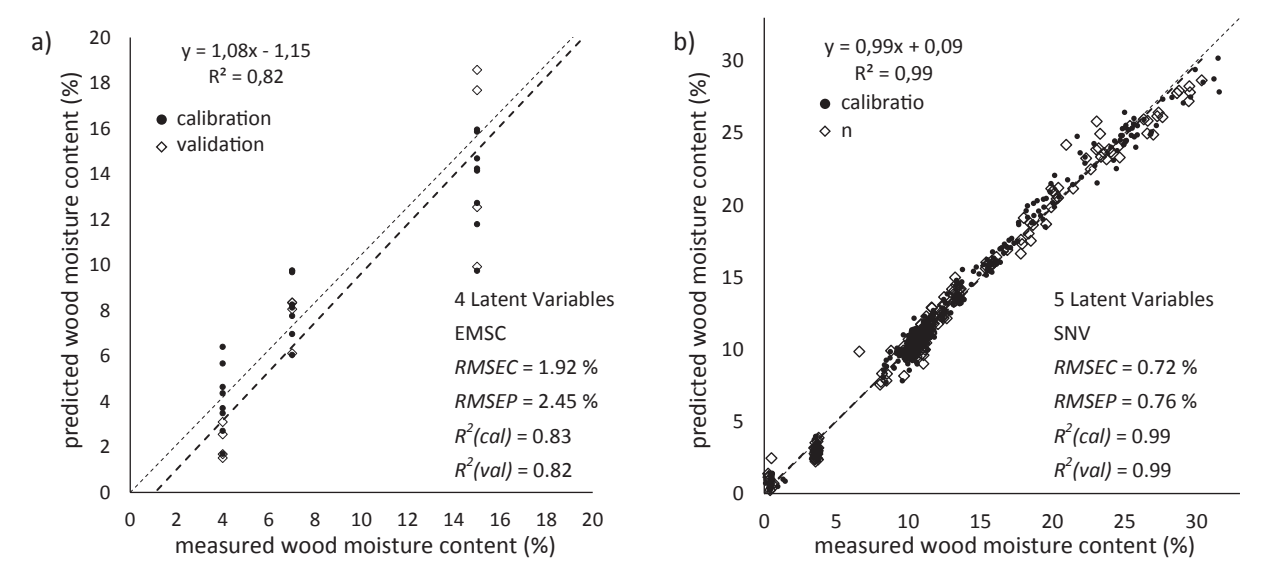


Fig. 10. PLS models for prediction of the beech wood moisture content using NIR spectroscopy based on experimental boards used for the gluing tests (a) and follow-up dedicated experimental campaign (b). Note: The regression dashed line corresponds to the validation data set (open diamonds) and the diagonal point line indicates the perfect correlation trend.

3.7. Total delamination

Evaluationg or even quantifying the delamination risk in gluelaminated timber structures is of the greatest interest for timberproducing industries, constructors as well as building operators [76]. The ultimate use of NIR spectra collected in this research was to link the glue bond performance assessed by the delamination test with the near infrared absorbance on the wood surface before applying adhesives. It is not a straightforward measurement as the delamination ratio depends on several factors, where the state of the wood surface before bonding is only one of those. It was impossible to integrate the combined effects of the gluing process with the chemometric model. For that reason, the open time between the application of adhesive and press closure, surrounding air temperature and relative humidity during glue application and pressing, pressure level and its distribution, curing time, among other factors, were not included as model variables. Finally, the variance to the delamination results associated with minor deviations of the test procedure varying between each sample lot was also neglected. Even with all the above-mentioned constraints, the chemometric model linking total glue bond delamination with NIR spectra was satisfactory. Samples from scenarios I, II and III were tested to minimize the unwanted source of variance focussing on the effect of planed wood characteristics. A clear differentiation between resistant (<25 % delamination) and weak (>75 % delamination) samples is evidenced in Fig. 11a. The PLS prediction model may be converted into discriminant analysis classifying wooden boards to different classes containing possibly problematic (high delamination) samples.

The total delamination ratio is a standardized quantifier of the glue bond performance. However, it is the only global value computed as an average of numerous measurements performed on six specimens containing five glue bonds each. An alternative delamination quantifier is the total delamination length computed separately for each glue line layer on all the samples from the same replica. This is expressed in millimetres and corresponds to the crack length assessed separately for

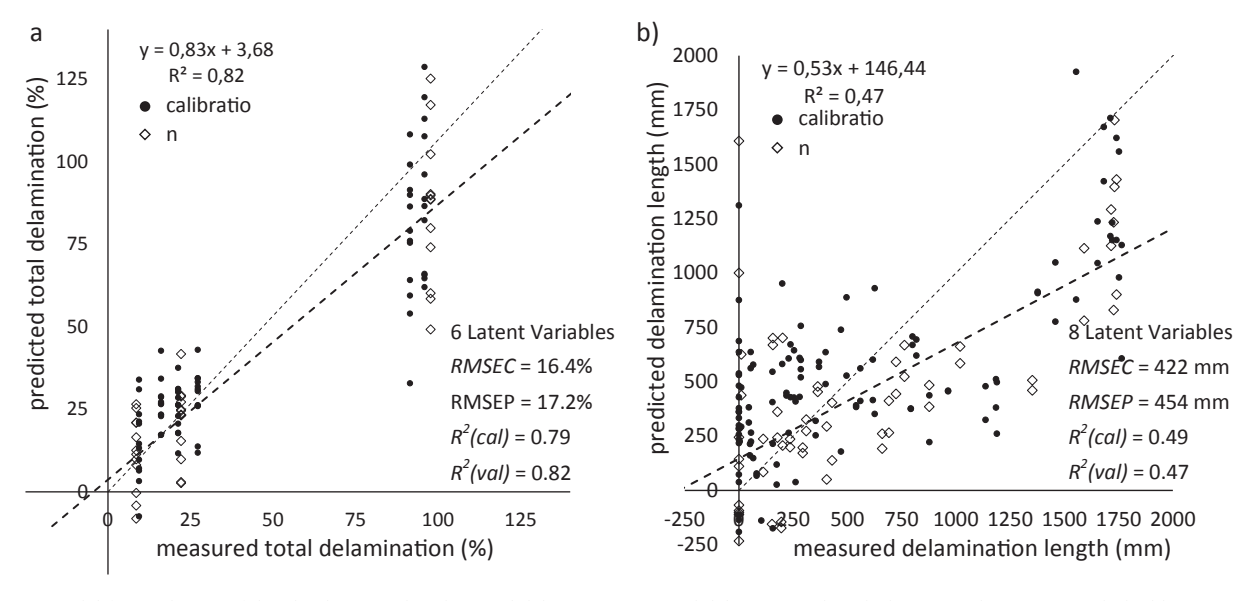


Fig. 11. PLS model for prediction of the glue-laminated timber total delamination (a) and delamination length (b). Note: The regression dashed line corresponds to the validation data set (open diamonds) and the diagonal point line indicates the perfect correlation trend.

each glued lamella. The delamination length can also be predicted by NIR spectroscopy. In that case, each bond line is assessed separately and related to the specific pair of two near infrared spectra acquired from both bonded surfaces. The resulting prediction model is presented in Fig. 11b. A higher scatter of results can be noticed, even if an optimal number of latent variables determined by cross-correlation was LV = 8. It was an effect of the broader samples set used for model generation including all wood samples from scenarios I, II, III, IV and V. The second derivative (Savitzky-Golay) was identified as an optimal spectra preprocessing. In analogy to the total delamination, an appropriate differentiation between resistant and weak bond lines can be assumed. It is clear that from its definition, the delamination cannot extend 100%. However, it may appear as an artefact when predicting the total delamination with chemometric models, as evidenced in Fig. 11a. Nevertheless, it is assumed that both models presented are suitable for in-factory screening of materials potentially problematic for gluelaminated timber production.

The series of chemometric models presented above are considered as proof-of-concept results for pilot industrial trials. The complete analysis of each model presented above, including loadings or detailed spectra interpretation, is limited due to the already extended size of this report. However, all the reference data used in the experimentation are available for download at the public data repository [77].

4. Conclusions

The above report allows generating a conclusion that the proof-of-concept experiment can be considered a success. The evaluated Micro-NIR sensor is a portable, resistant and easy-to-operate instrument. It allowed measuring>2500 spectra used for calibration of various chemometric models. The user interface is very easy to learn, and a direct assessment of wood properties is straightforward after integrating prediction models with the scanner software. A single measurement cycle takes less than 3 s, enabling this method to become an alternative routine quality assurance solution for off-line implementation at the production facility.

It is important to remember that from the definition, chemometric models are approximation and generalization of the data recorded in the spectra. It is a frequently neglected fact and, therefore, "not perfect" models are sometimes considered as a "failure". However, reliability of models tuned with a small number of reference data is low. It is especially the case of wood characterization where intrinsic variance between and within samples is very high. The number of data points used in this research was a compromise between the realistic size of measurement campaign and general objective of this research aiming to demonstrate suitability of NIR spectroscopy when implemented in the factory. The set of presented prediction models should be considered as a decent and trustworthy example of realistic solutions available with the portable spectroscopic instruments. The prediction capacity, even if far from perfection, allows fast screening of raw resources and provides approximate values not available till now by means of alternative to NIR fast and low-cost measurement procedures.

Even if not tested directly in this research, near infrared spectroscopy has great potential for the identification of wood imperfections that are not visible in current imaging systems, such as abnormal chemical composition, uneven moisture distribution or excessive content of extractive components. Unfortunately, due to limited access to the reference chemical analysis, it was not possible to demonstrate the MicroNIR sensor performance in the chemical composition analysis of wood used in this study. Nevertheless, the post-processing of collected NIR spectra allowed the generation of several chemometric models capable (with different degrees of accuracy) to predict diverse wood properties. As expected, the best performance was noticed for assessing wood moisture content, with a slightly weaker capacity to estimate wood density and mechanical properties. Even if the experiment was designed to cover a broad range of reference wood characteristics

assessed at a relatively large sample set, further focused tests may dramatically improve the prediction capacity of such a spectroscopic system. It was demonstrated in the case of wood moisture content prediction. The chemometric model performance was optimal when a sufficient number of representative samples covering a broad range of moisture content values was provided as a calibration set. The same improvement of performance is expected when an additional set of density and targeted MoE reference samples will be used for a betaversion of the PLS models' calibration.

NIR spectroscopy was moderately capable in the prediction of wood surface roughness. However, the wood surface characterization by means of the stylus technique, as tested here, is rather problematic. An alternative methodology, such as two-dimensional surface topography scanning using optical profilometers, should be implemented instead to reinvestigate the suitability of NIR spectroscopy for the prediction of roughness.

A great advantage of the near infrared system is its capacity to discriminate against wooden boards' provenance. It was demonstrated that the traceability of the raw resources is possible as well as the automatic classification of diverse wood defects. The same approach can also be extended for the screening of boards before gluing operation. The chemometric model presented in this report was capable of predicting the total delamination as well as detailed delamination length. Even with that, all chemometric models presented are "proof of concept" rather than ready-to-implement solutions compatible with industrial expectations. The number of cases and samples necessary for the consistent models' development is very high and can be scrutinized only along systematic studies performed at the specific factory.

Wood (surface) properties assessed in the presented research were predicted with NIR indirectly. This is a very common constrain when implementing this technology in any kind of applications. The mechanical properties (for example) are not directly assigned to specific molecular vibrations but are indirectly related to the chemical composition and physical properties of the wood polymer matrix. The pioneer implementation of the NIR spectroscopy toward prediction of the glue bond resistance is highly challenging. The resistance is associated with the properties of glued materials, but also other factors are highly influencing the performance, such as adhesive type, application, gluing process conditions, curing of the adhesive, as well as testing procedure, among other aspects. Even if all the efforts were directed to control the variance within the experiment, the natural variability of wood, combined with the manufacturing process variations can be an explanation of the not optimal determination coefficients R^2 . Although R^2 is a convenient quantifier of the regression, it is not the ultimate and unique parameter. There are several alternative descriptors used for describing prediction performance of chemometric models, such as root mean square errors, T^2 , Q-residuals, bias, RPD, among the others. The presented R^2 are not very high but corresponds to typically noticed values when statistically analysing biological materials, such as wood.

Some limitations of the experimental set-up should be considered before the further system development and following industrial integration:

- the scanning frequency of the MicroNIR sensor is relatively low (0.5 Hz), which allows only off-line scanning, with limited possibility for in-line quality assessment
- the sensor allows single point measurement with relatively broad surface area (5 × 5 mm²), therefore, enabling detecting of only selected defects of fairly large size
- frequent calibration of the sensor is necessary to assure superior sensor's performance it is recommended to manually perform white and dark reference scans every 10 min
- the increased number of internal scans (set as 100 in this test) increases signal-to-noise-ratio, but also extends the measurement time

The manual NIR spectroscopy assessment of wood quality before

gluing is a highly recommended solution for implementation in gluelaminated timber production plants. However, further improvement of the chemometric models and measurement routines is indispensable before the practical implementation of the presented solution. It includes refining predicting models' performance by enriching the reference data set with high variability samples, defining an automatic outlier elimination algorithm and validation of alternative to MicroNIR sensors.

CRediT authorship contribution statement

Jakub Sandak:Conceptualization, Methodology, Software, Validation, Formal analysis, Investigation, Data curation, Writing – original draft, Writing – review & editing, Visualization, Supervision, Project administration, Funding acquisition,Peter Niemz:Conceptualization, Methodology, Validation, Resources, Writing – review & editing, Supervision, Project administration, Funding acquisition,Andreas Hänsel: Validation, Resources, Writing – review & editing, Project administration, Funding acquisition,Juana Mai:Validation, Investigation, Writing – review & editing,Anna Sandak:Validation, Resources, Writing – review & editing.

Declaration of Competing Interest

The authors declare that they have no known competing financial interests or personal relationships that could have appeared to influence the work reported in this paper.

Acknowledgements

Authors are grateful to neue Holzbau AG, Lungern, Switzerland, and Henkel & Cie. AG, Sempach, Switzerland, for financial and technical support. Special thanks to Dr. Stefan Bockel of BFH for his assistance and valuable discussions. The authors gratefully acknowledge the European Commission for funding the InnoRenew project (grant agreement #739574) under the Horizon2020 Widespread-2-Teaming program, the Republic of Slovenia (investment funding from the Republic of Slovenia and the European Union's European Regional Development Fund) and infrastructural ARRS program IO-0035. Part of this work was conducted during the project BI-IT/18-20-007 and N1-0093, funded by ARRS, as well as CLICK DESIGN "Delivering fingertip knowledge to enable service life performance specification of wood" (No. 773324) supported under the umbrella of ERA-NET Cofund ForestValue by the Ministry of Education, Science and Sport of the Republic of Slovenia. ForestValue has received funding from the European Union's Horizon 2020 research and innovation programme.

References

- Milner Associates, Timber Engineering Notebook series. No. 8: Glued laminated timber structures, The Institution of Structural Engineers, London 2013.
- [2] Y. Weinand, Advanced Timber Structures: Architectural Designs and Digital Dimensioning, Birkhäuser, 2016.
- [3] A. Hänsel, J. Sandak, A. Sandak, J. Mai, P. Niemz, Selected previous findings on the factors influencing the gluing quality of solid wood products in timber construction and possible developments: a review, Wood Mater. Sci. Eng. (2021), https://doi. org/10.1080/17480272.2021.1925963.
- [4] N. Rogeau, P. Latteur, Y. Weinand, An integrated design tool for timber plate structures to generate joints geometry, fabrication toolpath, and robot trajectories, Autom. Constr. 130 (2021), 103875, https://doi.org/10.1016/j. autcon.2021.103875.
- [5] G. Mirzaei, B. Mohebby, G. Ebrahimi, Glulam beam made from hydrothermally treated poplar wood with reduced moisture induced stresses, Constr. Build. Mater. 135 (2017) 386–393.
- [6] EN 14080:2013 Timber structures. Glued laminated timber and glued solid timber
 Requirements. European Committee for Standardization, Brussels 2013.
- [7] B. Franke, F. Scharmacher, A. Müller, Assessment of the Glue-Line Quality in Glued Laminated Timber Structures, in Materials and Joints in Timber Structures, S. Aicher, H.W., Reinardt, H. Garrecht (Eds.), Springer Netherlands, 2014, pp. 395-404

- [8] A.A. Marra, Technology on wood bonding. Principles in practice, Van Norstrand Reinhold, New York, 1992.
- [9] C. Vanya, Damage problems in glued laminated timber, Drewno 55 (188) (2012) 115–128.
- [10] M. Knorz, Investigation of structurally bonded ash (Fraxinus excelsior L.) as influenced by adhesive type and moisture, PhD thesis, TU München 2015).
- [11] EN 391:2001 Glued laminated timber: delamination test of glue lines. European Committee for Standardization, Brussel 2001.
- [12] EN 302-1:2013 Adhesives for load-bearing timber structures Test methods Part 1: Determination of longitudinal tensile shear strength. European Committee for Standardization, Brussels.
- [13] T.R. Truax, M.L. Selbo, Results of accelerated tests and long-term exposures on glue joints in laminated beams, Trans. ASME 70 (1948) 393–400.
- [14] M.L. Selbo, Rapid evaluation of glue joints in laminated timbers, For. Prod. J. 14 (8) (1964) 361–365.
- [15] ASTM D2559 Standard specification for adhesives for structural laminated wood products for use under exterior (wet use) exposure conditions. ASTM International, West Conshohocken 2012.
- [16] EN 302-2:2017 Adhesives for load-bearing timber structures Test methods Part 2: Determination of resistance to delamination, European Committee for Standardization, Brussels 2017.
- [17] R. Vella, M.T. Heitzmann, A. Redman, H. Bailleres, Comparison of test methods for the determination of delamination in glued laminated timber, BioRes. 14 (4) (2019) 7920–7934.
- [18] E. Johansson, A. Svenningsson, Delamination of cross-laminated timber and its impact on fire development | Focusing on different types of adhesives, Environ Sci. Report (2018) 5562.
- [19] EN 1995-1-1:2004 Eurocode 5: Design of Timber Structures. Part 1-1: General Common rules and rules for buildings European Committee for Standardization, Brussel, 2004.
- [20] V. Angst-Nicollier, Moisture induced stresses in glulam. Trondheim: Diss. Norwegian University of Science and Technology, NTNU-Trondheim, 2012.
- [21] EN 1194:1999 Timber structures. Glued laminated timber. Strength classes and determination of characteristic values European Committee for Standardization, Brussel, 1999.
- [22] EN 385:2002. Finger jointed structural timber Performance requirements and minimum production requirements. European Committee for Standardization, Brussel. 2002.
- [23] EN 386:2002. Glued laminated timber Performance requirements and minimum production requirements. European Committee for Standardization, Brussel, 2002.
- [24] EN 301:2006. Adhesives, phenolic and aminoplastic, for load-bearing timber structures – Classification and performance requirements. European Committee for Standardization, Brussel, 2006.
- [25] EN 408:2010 Timber structures Structural timber and glued laminated timber Determination of some physical and mechanical properties. European Committee for Standardization. Brussel. 2010.
- [26] C.A. Aguilera, C. Aguilera, A.D. Sappa, Melamine faced panels defect classification beyond the visible spectrum, Sensors 18, 3644 (2018) 10pp.
- [27] T. Gergel, T. Bucha, M. Gejdoš, Z. Vyhnáliková, Computed tomography log scanning – high technology for forestry and forest based industry, Cent. Eur. For. J. 65 (2019) 51–59.
- [28] M. Dick Tech Update: Scanners and optimizers in 2020, Canadian Forest Industries, https://www.woodbusiness.ca/tech-update-scanners-and-optimizers-in-2020/ 2021, (accessed 03 May 2021).
- [29] O. Myronycheva, E. Sidorova, O. Hagman, M. Sehlstedt-Persson, O. Karlsson, D. Sandberg, Hyperspectral imaging surface analysis for dried and thermally modified wood: an exploratory study, J. Spectrosc. (2018) 10. ID 7423501.
- [30] B. Leblon, O. Adedipe, G. Hans, A. Haddadi, S. Tsuchikawa, J. Burger, R. Stirling, Z. Pirouz, K. Groves, J. Nader, A. LaRocque, A review of near-infrared spectroscopy for monitoring moisture content and density of solid wood, For. Chron. 89 (05) (2013) 595–606, https://doi.org/10.5558/tfc2013-111.
- [31] S. Tsuchikawa, A review of recent near-infrared research for wood and paper, Appl. Spectrosc. Rev. 42 (2007) 43–71.
- [32] C.L. So, B. Via, L.H. Groom, L.R. Schimleck, T.F. Shupe, S.S. Kelley, T.G. Rials, Near-infrared spectroscopy in the forest products industry, For. Prod. J. 54 (2004) 6–16.
- [33] L.R. Schimleck, C.A. Raymond, C.L. Beadle, G.M. Downes, P.D. Kube, J. French, Applications of NIR spectroscopy to forest research, Applia J. 53 (2000) 458–464.
- [34] J. Sandak, A. Sandak, R. Meder, Assessing trees, wood and derived products with NIR spectroscopy: hints and tips, J. Near Infrared Spectrosc. 24 (6) (2016) 485–505
- [35] A.C.M. Campos, P.R.G. Hein, R.F. Mendes, L.M. Mendes, G. Chaix, Near infrared spectroscopy to evaluate composition of agro-based particleboards, BioRes 4 (3) (2009) 1058–1069.
- [36] A. Sandak, J. Sandak, D. Janiszewska, S. Hiziroglu, M. Petrillo, P. Grossi, Prototype of the near-infrared spectroscopy expert system for particleboard identification, J. Spectrosc. (2018) 11. ID 6025163.
- [37] J. Sandak, A. Sandak, A. Zitek, B Hinterstoisser, G. Picchi, Development of low-cost portable spectrometers for detection of wood defects, Sensors 20, 2 (2020) 545 doi: 10.3390/s20020545.
- [38] R. Meder, W. Stahl, P. Warburton, S. Woolley, S. Earnshaw, K. Haselhofer, K. van Langenberg, N. Ebdon, R. Mulder, At-line validation of a process analytical technology approach for quality control of melamine-urea-formaldehyde resin in composite wood-panel production using near infrared spectroscopy, Anal. Bioanal. Chem. 409 (3) (2017) 763–771.

- [39] A. Taylor, B.K. Via, Potential of visible and near infrared spectroscopy to quantify phenol formaldehyde resin content in oriented strandboard, Eur. J. Wood Wood Prod. 67 (1) (2009) 3–5.
- [40] M. Gonçalves, N.T. Paiva, J.M. Ferra, J. Martins, F. Magalhães, L. Carvalho, Near infrared spectroscopy for rapid determination of solids content of amino resins, J.. Near Infrared Spectrosc. 28 (2020) 344–350.
- [41] F. Gaspar, J. Lopes, H. Cruz, M. Schwanninger, J. Rodrigues, Application of near infrared spectroscopy and multivariate data analysis for the evaluation of glue lines of untreated and copper azole treated laminated timber before and after ageing, Polym. Degrad. Stab. 94 (2009) 1061–1071.
- [42] N. Pemberger, C.W. Huck, L.K.H. Bittner, Using near-infrared spectroscopy to monitor the curing reaction of silicone adhesives, Spectrosc. Online 30 (8) (2015) 8-19
- [43] S.K. Tomlinson, O.R. Ghita, R.M. Hooper, K.E. Evans, The use of near-infrared spectroscopy for the cure monitoring of an ethyl cyanoacrylate adhesive, Vibr. Spectrosc. 40 (1) (2006) 133–141.
- [44] C. Biller, C.R. Hurburgh, N. Cao, G.R. Rippke, Calibration of the JDSU MicroNir 1700 for agricultural product analysis, NIR News 25 (6) (2014) 16.
- [45] C.A.T. Dos Santos, M. Lopo, R.N.M.J. Páscoa, J.A. Lopes, A review on the applications of portable near-infrared spectrometers in the agro-food industry, Appl. Spectrosc. 67 (2013) 1215–1233.
- [46] V. Barthet, M. Petryk, B. Siemens, Rapid nondestructive analysis of intact canola seeds using a handheld near-infrared spectrometer, J. Am. Oil Chem. Soc. 97 (2000) 577–589.
- [47] S. Grassi, E. Casiraghi, C. Alamprese, Handheld NIR device: a non-targeted approach to assess authenticity of fish fillets and patties, Food Chem. 243 (2018) 382–388
- [48] M.D. Neves, R. Poppi, H. Siesler, Rapid determination of nutritional parameters of pasta/sauce blends by handheld near-infrared spectroscopy, Molecules, 24, 11 (2019) 2029. doi: 10.3390/molecules24112029.
- [49] M. Rani, C. Marchesi, S. Federici, G. Rovelli, I. Alessandri, I. Vassalini, S. Ducoli, L. Borgese, A. Zacco, F. Bilo, E. Bontempi, L.E. Depero, Miniaturized Near-Infrared (MicroNIR) spectrometer in plastic waste sorting, Materials 12 (2019) 2740, https://doi.org/10.3390/ma12172740.
- [50] H. Yan, H.W. Siesler, Identification performance of different types of handheld near-infrared (NIR) spectrometers for the recycling of polymer commodities, Appl. Spectrosc. 72 (2018) 1362–1370.
- [51] H. Parastar, G. van Kollenburg, Y. Weesepoel, A. van den Doel, L. Buydens, J. Jansen, Integration of handheld NIR and machine learning to "Measure & Monitor" chicken meat authenticity, Food Control 112 (2020), 107149.
- [52] https://www.viavisolutions.com/en-us/osp/products/micronir-onsite-w (accessed 03 May 2021).
- [53] H. Martens, E. Stark, Extended multiplicative signal correction and spectral interference subtraction: new preprocessing methods for near infrared spectroscopy, J. Pharm. Biomed. Anal. 9 (1991) 625–635.
- [54] S. Wold, H. Antti, F. Lindgren, J. Öhman, Orthogonal signal correction of near-infrared spectra, Chemom. Intell. Lab. Syst. 44 (1–2) (1998) 175–185, https://doi.org/10.1016/S0169-7439(98)00109-9.
- [55] A. Savitzky, M. Golay, Smoothing and differentiation of data by simplified least squares procedures, Anal. Chem. 36 (8) (1964) 1627–1639.
- [56] V. Bucur, Delamination in Wood, Wood Products and Wood-Based Composites, Springer, New York, 2011.
- [57] G. Kandler, M. Lukacevic, J. Füssl, Experimental study on glued laminated timber beams with well-known knot morphology, Eur. J. Wood Wood Prod. 76 (5) (2018) 1435–1452

- [58] P.D. Jones, L.R. Schimleck, G. Peter, R. Daniels, A. Clark, Non-destructive estimation of Pinus taeda L. wood properties for samples from a wide range of sites in Georgia, Can. J. For. Res. 35 (2005) 85-92.
- [59] L.R. Schimleck, C. Mora, R. Daniels, Estimation of the physical wood properties of green *Pinus taeda* radial samples by near-infrared spectroscopy, Can. J. For. Res. 33 (2003) 2297–2305.
- [60] L.R. Schimleck, R. Evans, J. Llic, Estimation of Eucalyptus delegatensis wood properties by near-infrared spectroscopy, Can. J. For. Res. 31 (2001) 1671–1675.
- [61] M. Defo, M. Taylor, B. Bond, Determination of moisture content and density of fresh-sawn red oak lumber by near-infrared spectroscopy, For. Prod. J. 57 (5) (2007) 68–72.
- [62] P. Hoffmeyer, J.G. Pedersen, Evaluation of density and strength of Norway spruce wood by near-infrared reflectance spectroscopy, Holz. Roh. Werkst. 53 (1995) 165–170.
- [63] W. Gindl, M. Schwanninger, B. Hinterstoisser, A. Teischinger, The relationship between near-infrared spectra of radial wood surfaces and wood mechanical properties, J. Near Infrared Spectrosc. 9 (2001) 255–261.
- [64] W. Ni, L. Nørgaard, M. Mørup, Non-linear calibration models for near infrared spectroscopy, Anal. Chim. Acta 27 (813) (2015) 1–14.
- [65] L.R. Schimleck, J.L. Matos, R. Trianoski, J.G. Prata, Comparison of methods for estimating mechanical properties of wood by NIR spectroscopy, Spectroscopy (2018) 1-10
- [66] C. Söğütlü, Determination of the effect of surface roughness on the bonding strength of wooden materials, BioRes. 12 (1) (2017) 1417–1429.
- [67] Z. Ahmad, W.C. Lum, S.H. Lee, M.A. Razlan, W.H.W. Mohamad, Mechanical properties of finger jointed beams fabricated from eight Malaysian hardwood species, Constr. Build. Mater. 145 (2017) 464–473.
- [68] S. Tiryaki, A. Malkocoglu, S. Ozsahin, Using artificial neural networks for modeling surface roughness of wood in machining process, Constr. Build. Mater. 66 (2014) 320, 335
- [69] J. Sandak, C. Tanaka, Evaluation of surface smoothness by laser displacement sensor 1: Effect of wood species, J. Wood Sci. 49 (4) (2003) 305–311.
- [70] Z.W. Zhong, S. Hiziroglu, C.T.M. Chan, Measurement of the surface roughness of wood based materials used in furniture manufacture, Measurement 46 (4) (2013) 1482–1487.
- [71] S.J. Sanabria, C. Mueller, J. Neuenschwander, P. Niemz, U. Sennhauser, Air-coupled ultrasound as an accurate and reproducible method for bonding assessment of glued timber, Wood Sci. Technol. 45 (2011) 645–659.
- [72] S.J. Sanabria, R. Furrer, J. Neuenschwander, P. Niemz, U. Sennhauser, Air-coupled ultrasound inspection of glued laminated timber, Holzforschung 65 (2011) 377–387
- [73] A. Morin-Bernard, P. Blanchet, C. Dagenais, A. Achim, Glued-laminated timber from northern hardwoods: effect of finger-joint profile on lamellae tensile strength, Constr. Build. Mater. 271 (2021), 121591.
- [74] C.R. Avila, J. Ferré, R.R. de Oliveira, A. de Juan, W.E. Sinclair, F.M. Mahdi, A. Hassanpour, T.N. Hunter, R.A. Bourne, F.L. Muller, Process monitoring of moisture content and mass transfer rate in a fluidised bed with a low cost inline MEMS NIR sensor. Pharm. Res. 37 (2020) 84.
- [75] A. Sandak, J. Sandak, M. Riggio, Estimation of physical and mechanical properties of timber members in service by means of infrared spectroscopy, Constr. Build. Mater. 2 (2015) 1197–1205.
- [76] J. Gomes Ferreira, H. Cruz, R. Silva, Failure behaviour and repair of delaminated glulam beams, Constr. Build. Mater. 154 (2017) 384–398.
- [77] J. Sandak, NIR spectra collected along the glue-laminated timber production: Zenodo dataset (2021). doi: 10.5281/zenodo.4736103.